

POP: Online Structural Pruning Enables Efficient Inference of Large Foundation Models

Yi Chen¹ Wonjin Shin¹ Shuhong Liu² Tho Mai¹ Jeongmo Lee¹
 Chuanbo Hua¹ Kun Wang¹ Jun Liu³ Joo-Young Kim¹

Abstract

Large foundation models (LFMs) achieve strong performance through scaling, yet current structural pruning methods derive fixed pruning decisions during inference, overlooking sparsity patterns that emerge in the autoregressive token generation. In this paper, we propose POP (Partition-guided Online Pruning), an efficient online structural pruning framework that enables context-conditioned dynamic pruning with minimal computational overhead. POP partitions model channels into retained, candidate, and pruned regions, where prefilling defines a coarse pruning partition, and the decoding stage generates a fine-grained mask within the candidate region, avoiding full-channel re-evaluation. The coarse pruning partition preserves consistently important weights, while the fine-grained masking provides context-conditioned variation during decoding. Moreover, POP is a lightweight, plug-and-play method that requires no preprocessing, including offline calibration, retraining, or learning predictors. Extensive evaluations across diverse LFM, including large language models (LLMs), mixture-of-experts models (MoEs), and vision–language models (VLMs), demonstrate that POP consistently delivers higher accuracy than existing pruning approaches while incurring smaller computational overhead and minimizing inference latency.

1. Introduction

Large foundation models (LFMs) (Bommasani, 2021), such as large language models (LLMs) (Brown et al., 2020; Chowdhery et al., 2023), vision–language models (VLMs) (Radford et al., 2021; Alayrac et al., 2022), and

¹Korea Advanced Institute of Science and Technology (KAIST), Daejeon, South Korea ²University of Tokyo, Tokyo, Japan ³Tokyo Institute of Technology, Tokyo, Japan. Correspondence to: Joo-Young Kim <jooyoung1203@kaist.ac.kr>.

Preprint. February 9, 2026.

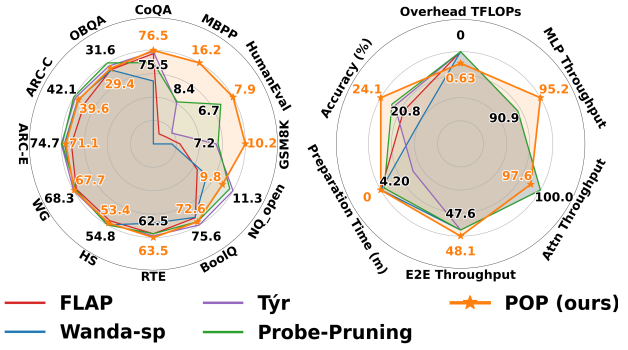


Figure 1. Task-wise normalized performance across benchmarks on Llama2-7B, together with inference efficiency. POP exhibits more consistent performance across tasks while maintaining higher efficiency than baseline pruning methods.

mixture-of-experts models (MoE) (Du et al., 2022; Fedus et al., 2022; Liu et al., 2024), have achieved remarkable performance gains through continuous scaling of model size (Kaplan et al., 2020). However, this scaling trend comes with substantial computational overhead, posing a major challenge for efficient inference. To mitigate this issue, various model compression techniques (Han et al., 2015a), such as quantization (Jacob et al., 2018; Dettmers et al., 2022), low-rank decomposition (Denton et al., 2014; Hu et al., 2022), and pruning (Han et al., 2015b;a; Sun et al., 2024), have been extensively studied. Among them, structural pruning (An et al., 2024; Li et al., 2025; Ma et al., 2023; Le et al., 2025) is particularly appealing, as it removes entire computational structures (e.g., weight channels) without relying on specialized hardware support (Wang et al., 2020; Xia et al., 2022; Hu et al., 2025).

Early structural pruning methods for LLMs typically derive a static pruning mask through offline calibration (Ma et al., 2023; An et al., 2024; Li et al., 2025) or pretrained predictors (Liu et al., 2023), and apply it uniformly throughout inference. Although effective at reducing model size and computational cost, such static strategies are input-agnostic and fail to capture the diverse sparsity patterns induced by different contexts and tasks. Recent studies have therefore explored context-conditioned (Hou et al., 2025; Le et al., 2025) or dynamic pruning (Liu et al., 2025a) approaches

that adapt pruning decisions across input prompts, often without retraining.

Despite this progress, online pruning remains challenging. Most existing approaches make pruning decisions only once during the prefilling stage and apply the resulting decision throughout autoregressive generation. Such static pruning strategies fail to adapt to evolving decoding contexts, which can conflict with the inherently input-dependent computation behavior of LLMs and result in substantial performance degradation on generation tasks compared to dense models. This issue is reflected in our empirical observations. For example, under a 20% pruning ratio, the model pruned by the static framework Tyr (Li et al., 2025) retains 98% accuracy on short-form QA tasks such as ARC-C (Clark et al., 2018), with LLaMA-2-7B (Touvron et al., 2023), but preserves only 35% performance on long-form generation benchmarks such as MBPP (Austin et al., 2021). These observations motivate the consideration of alternatives to static pruning, raising the following question:

Can pruning decisions be conditioned on the generation context during online inference?

A natural way to address this question is to update pruning decisions dynamically during decoding. However, most existing context-conditioned pruning methods are designed for multi-token settings. For example, Probe Pruning (Le et al., 2025) relies on probing-based importance estimation, while Instruction-Following Pruning (Hou et al., 2025) employs an input-conditioned predictor; both require aggregated activations across multiple tokens. Such designs are fundamentally incompatible with autoregressive decoding, where only a single token is available at each step. Even if one applies probing-based importance estimation to the generated token itself, it would further introduce an additional forward pass, incurring prohibitive runtime overhead. These limitations highlight the need for an online pruning framework that enables context-conditioned adaptation with minimal overhead and broad applicability across tasks and model architectures.

To narrow the performance gap between pruned and dense models while maintaining minimal runtime overhead, we propose POP (Partition-guided Online Pruning). POP is an online structural pruning framework that performs context-conditioned pruning decisions during autoregressive inference with negligible additional computation. In particular, POP is a lightweight and plug-and-play approach, requiring no preprocessing such as offline calibration, retraining, or predictor learning, and can be readily applied to diverse large foundation models. The main contributions of this work are summarized as follows:

- **We identify the necessity of online pruning during autoregressive generation.** We show that pruning de-

cisions fixed during prefilling introduce systematic bias in newly generated tokens because they remain determined by the initial prompt, highlighting the need for online, dynamic pruning to address contextual sparsity during decoding.

- **We propose POP: a Partition-guided Online Pruning framework that balances accuracy and efficiency.** POP introduces a tri-state channel partition based on prefilling-stage importance, dividing channels into retained, pruned, and candidate regions, where only candidate channels are dynamically selected during decoding, enabling fine-grained context adaptivity with minimal overhead.
- **We develop POP as a model-agnostic and deployment-friendly framework.** Without offline calibration, auxiliary predictors, or retraining, POP can be seamlessly applied to a wide range of LFs, enabling practical, scalable inference-time acceleration.

We empirically evaluate POP on diverse LFs, including representative LLMs, MoE models, and VLMs, and observe consistent accuracy gains and lower latency over state-of-the-art structural pruning methods. In particular, POP improves Llama3.1-8B by 5.27 on short-form QA and 17.71 on generation. Moreover, with only 2.85% FLOPs overhead relative to the dense model, POP achieves a 1.29× inference speedup on Llama2-7B.

2. Related Work

2.1. Contextual Sparsity in LLMs

LLMs exhibit contextual sparsity in internal computation, where only a subset of neurons is activated under a given input context (Michel et al., 2019; Geva et al., 2021; Bills et al., 2023; Luo et al., 2025). This property has motivated conditional-execution methods that dynamically select computation structures via learned predictors or input-adaptive thresholding. Deja Vu (Liu et al., 2023) employs per-layer predictors to activate a subset of attention heads and MLP neurons, with subsequent works improving the robustness of predictor-based sparsity (Akhauri et al., 2024). In parallel, training-free thresholding approaches induce sparsity by suppressing low-utility activations in an input-dependent manner (Lee et al., 2024; Zhou et al., 2024; Liu et al., 2025b). System- and architecture-level efforts further exploit this property for efficient inference and sparsity-aware design (Song et al., 2024; Mirzadeh et al., 2024).

MoE architectures instantiate contextual sparsity at a coarser granularity by replacing parts of the dense feed-forward computation with multiple experts and using a learned router to select only a small subset of experts for each token (Lepikhin et al., 2021; Zhou et al., 2022). This design yields

conditional computation, enabling parameter scaling while keeping per-token FLOPs roughly bounded by the number of activated experts (Dikkala et al., 2023).

2.2. Unstructured & Structural Pruning

Model weight pruning compresses LLMs by removing parameters while preserving accuracy. Unstructured pruning achieves high sparsity with limited post-training recovery: SparseGPT (Frantar & Alistarh, 2023) performs one-shot reconstruction-based pruning, while Wanda (Sun et al., 2024) adopts activation-informed saliency, with subsequent methods improving layer- or blockwise sparsity allocation (Xu et al., 2024; Yin et al., 2025). However, irregular sparsity often yields limited latency gains on mainstream GPUs, due to poor compatibility with dense kernels in the absence of specialized sparse runtimes.

Structured pruning removes contiguous architectural components, offering more predictable acceleration on standard hardware (Wang et al., 2020; Xia et al., 2022; Hu et al., 2025). LLM-Pruner (Ma et al., 2023) prunes coupled substructures with lightweight tuning, and LoRAPrune (Zhang et al., 2024b) integrates structured removal with low-rank adaptation (Hu et al., 2022). SliceGPT (Ashkboos et al., 2024) and ZipLM (Kurtić et al., 2023) further align pruning decisions with dense inference efficiency. For stronger compression, Sheared-LLaMA (Xia et al., 2024) combines structured pruning with continued training. Beyond static policies, recent methods explore adaptive sparsity allocation across layers or blocks (Zhong et al., 2025; Zhang et al., 2024c; Men et al., 2024; Yang et al., 2025b; He & Lin, 2025), including FLAP (An et al., 2024), which uses fluctuation-based criteria. Global optimization approaches (Li et al., 2025) employ evolutionary search to identify model-wide sparsity distributions under constrained budgets.

2.3. Context-Conditioned Pruning

Context-conditioned pruning adapts the pruning mask to each input, rather than applying a single context-agnostic mask after compression. EBERT (Liu et al., 2021) is an early method that dynamically prunes structured components using a lightweight input-conditioned predictor. Recent work revisits this paradigm for modern LLMs and extends the conditioning signal and optimization targets. Instruction-Following Pruning (Hou et al., 2025) learns an instruction-conditioned mask predictor and jointly optimizes it with the LLM so that different instructions activate different parameter subsets. Probe Pruning (Le et al., 2025) estimates batch-specific importance via lightweight probing and then applies online structured pruning for the remaining inference. Subsequent studies introduce alignment-aware constraints to stabilize dynamic masking under distribution shift (Patel et al., 2025). RAP (Liu et al., 2025a) formu-

Table 1. Comparison of pruning methods. Our approach prunes based on contextual input at inference time, requiring neither calibration nor additional training overhead.

Method	w/o.SFT	w/o.Calib	w/o.Predictor	Context-Cond.
LLM-Pruner	✗	✗	✗	✗
SparseGPT	✓	✗	✓	✗
Wanda	✓	✗	✓	✗
FLAP	✓	✗	✓	✗
Týr-the-Pruner	✓	✗	✓	✗
Deja vu	✓	✗	✗	✓
IF-Pruning	✗	✗	✗	✓
SkipGPT	✗	✓	✗	✓
Probe Pruning	✓	✗	✓	✓
Ours	✓	✓	✓	✓

lates runtime pruning as a control problem and uses an RL agent to adapt pruning decisions under memory budgets that couple model weights and KV-cache. μ -MoE (Koike-Akino et al., 2025) casts prompt-adaptive test-time pruning as micro-grained expert selection, enabling per-prompt structured sparsity without committing to a single mask.

3. Method

The objective of POP is to offer online structural pruning at inference time to improve computational efficiency and minimize latency while preserving accuracy. The comparisons between POP and previous works are listed in Table 1. We begin with the preliminaries of structural pruning and LLM architectures in Section 3.1. Motivated by the contextual sparsity of LFs, we empirically show the correlation of pruning partitions and formulate POP in Section 3.2. Section 3.3 subsequently elaborates our pruning metric. Section 3.4 analyzes pruning ratios and computation overhead.

3.1. Preliminaries and Notations

Notation. We denote a linear transformation by a weight matrix $\mathbf{W} \in \mathbb{R}^{C_{\text{out}} \times C_{\text{in}}}$, where C_{in} and C_{out} indicate the input and output channel dimensions, respectively. Let $\mathbf{X} \in \mathbb{R}^{B \times L \times C_{\text{in}}}$ denote the input activations, where B is the batch size and L is the sequence length. During autoregressive decoding, the activation at step t is denoted as $\mathbf{X}_t \in \mathbb{R}^{B \times 1 \times C_{\text{in}}}$. We use i to index output channels and k to index input channels. Channel-wise importance scores are denoted by I_i , and their step-wise counterparts during decoding are written as $I_i(t)$. The target pruning ratio is denoted by r .

Weight-Activation Structural Pruning. We consider the common activation-aware formulation for structural pruning, where importance is estimated jointly from model weights and input activations (Sun et al., 2024). The element-wise

importance weight can be defined as

$$I_{i,k} = |W_{i,k}| \cdot \|\mathbf{X}_k\|_2, \quad (1)$$

where $\|\mathbf{X}_k\|_2$ denotes the ℓ_2 norm of activations of the k -th input channel aggregated across tokens and samples.

While importance can be computed for individual weights, structural pruning operates on channel-level structures rather than isolated parameters. Accordingly, following (An et al., 2024), element-wise importance scores are aggregated to obtain output-channel importance, which can be defined as

$$I_i^{\text{out}} = \mathcal{A}(\{I_{i,k}\}_{k=1}^{C_{\text{in}}}), \quad i = 1, \dots, C_{\text{out}}, \quad (2)$$

where $\mathcal{A}(\cdot)$ denotes an aggregation operator that maps element-wise scores to a channel-level importance value.

The resulting output-channel importance vector \mathbf{I}^{out} serves as the basic criterion for structural pruning, where pruning decisions are applied to entire channels as a unit. In feed-forward networks (FFNs), each output channel corresponds to one dimension of the intermediate representation, which is consistently used across consecutive linear transformations. Therefore, output-channel importance provides a principled basis for structural pruning of FFN blocks.

3.2. Contextual Sparsity for Online Pruning

As discussed in the preliminaries, importance estimation in LFMIs depends jointly on fixed model weights and input-dependent activation statistics. During inference, this coupling induces a structural mismatch: pruning targets remain fixed at the channel level, whereas the activation patterns used for importance estimation vary across inference stages. In particular, while prefilling computes importance from full-sequence activations of the input prompt, decoding relies on step-wise activations \mathbf{X}_t , in which the effective token context collapses from length L to a single token, leading to token-dependent fluctuations in channel importance.

Figure 2 provides a direct visualization of this phenomenon. Channels are sorted according to their importance ranking obtained at the prefilling stage, and their relative rankings at each decoding step are tracked thereafter. As illustrated in Figure 2(a), channel rankings exhibit noticeable temporal variations during decoding, yet the overall ordering remains strongly anchored to the prefilling reference. This behavior is further quantified in Figure 2(b). The mean rank difference reflects the degree of fine-grained ranking variation across decoding steps, while the Top-50% channel overlap measures the stability of highly important channels. Across both GSM8K and MBPP, we observe that although local ranking perturbations persist, a substantial portion of top-ranked channels remains consistent throughout decoding.

Together, these observations reveal a characteristic pattern of decoding-time behavior: global importance structure re-

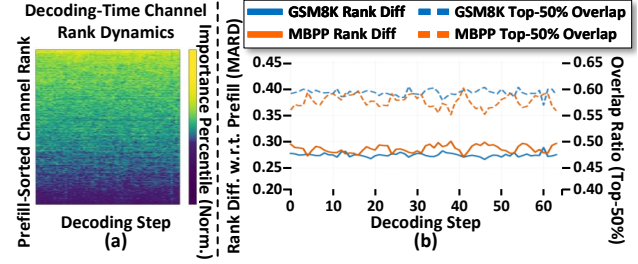


Figure 2. Decoding-time structural dynamics under online pruning. (a) Channel-rank evolution across decoding steps, where channels are ordered by their prefilling-stage importance and colors indicate normalized rank percentiles. (b) Mean rank difference and Top-50% channel overlap with respect to the prefilling ranking on the generation benchmarks GSM8K and MBPP using Llama3.1-8B, reflecting the degree of ranking variation and the stability of highly important channels during decoding.

mains largely stable, whereas intermediate channels exhibit context-dependent fluctuations. We refer to this coexistence of structural stability and localized variation as *contextual sparsity*. As a result, pruning decisions determined solely at the prefilling stage are insufficient to fully capture decoding-time computation, motivating the need for online structural pruning that adapts pruning decisions to the evolving generation context.

3.3. POP Architecture

Motivated by the contextual sparsity observed above, we design POP as a two-stage online pruning framework that separates coarse-grained pruning decisions from fine-grained, context-conditioned pruning during autoregressive decoding. The overview of POP is illustrated in Figure 3 (a) and (b). We focus on pruning FFNs, which dominate the model size as shown in Figure 3(d), while the proposed framework can be extended to other components such as attention heads.

Calibration Stage. Unlike previous approaches (Sun et al., 2024; An et al., 2024; Le et al., 2025; Li et al., 2025) that require offline calibration, shown in Figure 3 (e), POP is a plug-and-play framework that requires no preparation or training, and is ready for out-of-the-box inference.

Prefilling Stage. Inference begins with the *prefilling* stage, which processes all prompt tokens in parallel and produces full-sequence activations $\mathbf{X} \in \mathbb{R}^{B \times L \times C_{\text{in}}}$. These activations offer a global view of channel utilization under the given input prompt. Leveraging this information, POP derives an initial *coarse pruning partition*. Channel-wise importance scores I_i^{out} are computed from the full input prompt \mathbf{X} , following the formulation in Section 3.1.

Given a target pruning ratio r and a partition width δ , POP defines a narrow importance band around the prun-

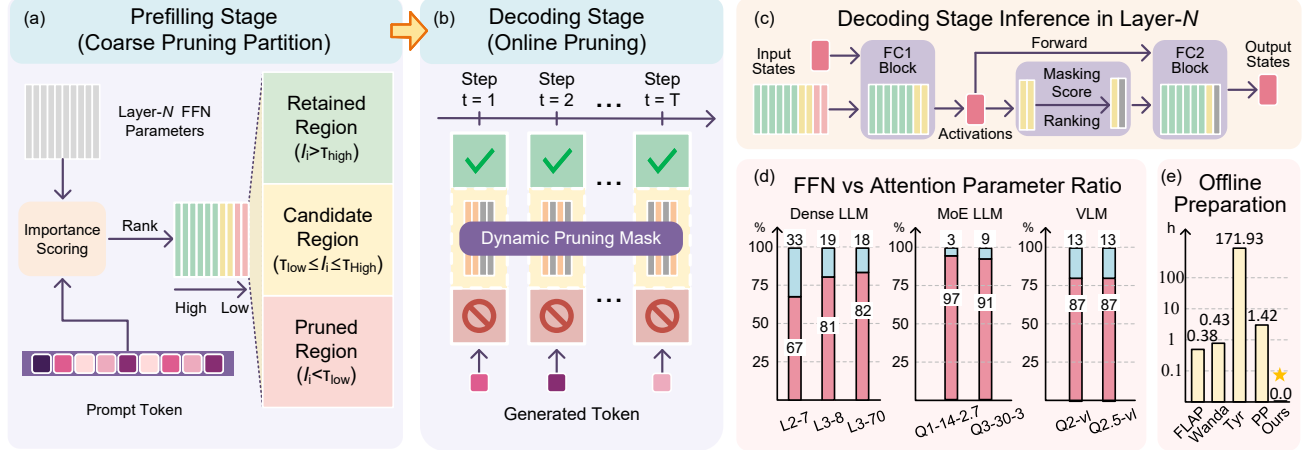


Figure 3. The overview of Partition-guided Online Pruning (POP). (a) During the prefilling stage, FFN channels in each layer are ranked by importance and partitioned into retained, candidate, and pruned regions, forming a coarse pruning partition. (b) During decoding, POP performs online pruning by dynamically selecting candidate channels at each generation step using step-wise pruning masks. (c) At each decoding step, intermediate activations are used to compute importance scores of candidates and update the pruning mask before the final FFN computation in layer N . (d) The proportion of FFN parameters dominates over attention parameters across dense LLMs, MoE LLMs, and VLMs, motivating our FFN-focused pruning. (e) Compared with prior methods, POP requires no offline preparation cost.

ing threshold. Let $q_\alpha(\cdot)$ denote the α -quantile of the importance scores $\{I_i^{\text{out}}\}_{i=1}^{C_{\text{out}}}$. Two thresholds are defined as $\tau_{\text{low}} = q_{r-\delta}$ and $\tau_{\text{high}} = q_{r+\delta}$. Channels are then partitioned into three disjoint regions:

- **Retained Region (\mathcal{R}):** $\mathcal{R} = \{i \mid I_i^{\text{out}} \geq \tau_{\text{high}}\}$. Channels in this region exhibit consistently high importance and are always preserved, forming a stable computational backbone throughout inference.
- **Pruned Region (\mathcal{P}):** $\mathcal{P} = \{i \mid I_i^{\text{out}} \leq \tau_{\text{low}}\}$. These channels contribute marginally and are removed upfront to improve inference efficiency for the given input prompt.
- **Candidate Region (\mathcal{C}):** $\mathcal{C} = \{i \mid \tau_{\text{low}} < I_i^{\text{out}} < \tau_{\text{high}}\}$. This region captures channels with context-conditioned variability and defines a bounded *dynamic search space* for online pruning.

Decoding Stage. Following the prefilling stage, autoregressive models proceed one token at a time in the decoding stage, with each step producing activations $\mathbf{X}_t \in \mathbb{R}^{B \times 1 \times C_{\text{in}}}$. At each decoding step t , POP performs fine-grained, context-conditioned pruning within the candidate region. Given the step-wise activation \mathbf{X}_t , channel importance scores $I_i^{\text{out}}(t)$ are evaluated only for channels $i \in \mathcal{C}$, while channels in \mathcal{R} remain active and channels in \mathcal{P} remain disabled. By preserving the retained region and avoiding global importance re-evaluation, POP reduces the online overhead of pruning without degrading inference performance.

Based on the step-wise importance scores $I_i^{\text{out}}(t)$ evaluated for channels $i \in \mathcal{C}$, POP selects a subset of candidate chan-

nels such that the total number of active channels matches the target pruning ratio r . This step enables fine-grained, context-conditioned pruning, as channel selection is adaptively determined by the decoding context. The selected channels are then combined with the retained region to form the effective computation graph for decoding step t .

3.4. Pruning Metric and Inference Efficiency

In POP, we adopt activation-aware importance metrics following prior structural pruning methods such as Wanda (Sun et al., 2024) and Probe Pruning (Le et al., 2025). Rather than proposing new importance formulations, we focus on enabling their efficient online use during inference.

Given activations \mathbf{X} and a linear transformation parameterized by \mathbf{W} , the importance of the i -th output channel is computed as

$$I_i(\mathbf{X}) = \|\mathbf{W}_{:,i} \odot \mathbf{s}\|_2, \quad \mathbf{s}_k = \|\mathbf{X}_{:,:,k}\|_2, \quad (3)$$

which reflects the joint contribution of activation magnitude and associated weights.

The same importance formulation is used throughout inference. During prefilling, importance is first estimated from full-sequence or partial probing prompt activations to determine coarse pruning decisions. The prefilling inference is then completed under the resulting pruning structure, which is shared with the subsequent decoding stage.

To balance estimation accuracy and online efficiency, POP performs decoding in two steps. Retained and candidate channels first participate in the forward computation, yielding intermediate activations $\mathbf{H}_t = f(\mathbf{X}_t; \mathcal{R} \cup \mathcal{C})$. Step-wise

importance scores $I_i(t)$ are then evaluated from \mathbf{H}_t for channels $i \in \mathcal{C}$. Based on $I_i(t)$, a subset of candidate channels is selected in a context-dependent manner. Only the retained channels and the selected candidates are involved in the final computation for the current decoding step.

4. Experiment

Large Foundation Models. Our evaluation spans dense LLMs, VLMs, and MoE models. For dense large language models, we consider Llama-2 7B/13B/70B (Touvron et al., 2023), Llama-3.1 8B/70B (Dubey et al., 2024), and Qwen-3 8B/32B (Yang et al., 2025a). To examine MoE architectures, we include Qwen1.5-MoE-A2.7B (Team, 2024), Qwen2-57B-A14B (Yang et al., 2024), and Qwen3-30B-A3B (Yang et al., 2025a). VLMs are represented by Qwen2-VL (Wang et al., 2024) and Qwen2.5-VL (Bai et al., 2025). Additional experiments on pure vision backbones from SAM (Kirillov et al., 2023) are reported in the Appendix B.

Evaluation Benchmarks. We conduct our evaluations using the LM-Evaluation-Harness framework (Gao et al., 2024) for LLMs and MoE models, and the LMMs-Eval framework (Zhang et al., 2024a) for VLMs. The benchmarks are grouped into three categories according to their input modalities and inference characteristics: (i) **question answering (QA)** benchmarks for evaluating language understanding in LLMs and MoEs, (ii) **generation** benchmarks that require extended autoregressive inference, and (iii) **visual question answering (VQA)** benchmarks for assessing multimodal reasoning in VLMs. The QA benchmarks include BoolQ (Clark et al., 2019), RTE (Poliak, 2020), HellaSwag (Zellers et al., 2019), WinoGrande (Sakaguchi et al., 2019), ARC-Easy (Clark et al., 2018), ARC-Challenge (Clark et al., 2018), and OpenBookQA (Mihaylov et al., 2018). These tasks primarily evaluate model understanding and reasoning capability under limited-output inference settings. The text generation benchmarks include CoQA (Reddy et al., 2019), MBPP (Austin et al., 2021), NQ-Open (Kwiatkowski et al., 2019), HumanEval (Chen et al., 2021), and GSM8K (Cobbe et al., 2021), which require multi-step autoregressive generation and thus provide a more challenging testbed for decoding-stage efficiency. The VQA benchmarks include POPE (Li et al., 2023), OK-VQA (Marino et al., 2019), GQA (Hudson & Manning, 2019), ScienceQA (Lu et al., 2022), and MME (Fu et al., 2025). The evaluation metrics used for benchmarks are detailed in Appendix A.4, and the complete results corresponding to each table are provided in Appendix C. In addition, perplexity-based evaluations are reported in Appendix A.3.

Baseline Methods. We evaluate our method against recent structural pruning baselines, including Wanda (Sun et al., 2024), FLAP (An et al., 2023), and Týr (Li et al., 2025),

which rely on offline pruning, as well as Probe Pruning (Le et al., 2025), which supports online pruning. For Wanda, we adopt its structural pruning variant, denoted as Wanda-sp. The detailed settings for the offline stage of these baselines are provided in the Appendix A.2.

Implementation Details. We implemented all baseline methods strictly following their original designs. γ in POP for the partition fraction was set to 0.1. All experiments were conducted on RTX A6000 clusters, and the batch size is set to 10 for LLM evaluations and 1 for VLM evaluations. Since our method exclusively prunes FFN layers while preserving attention mechanisms, we adjust the pruning ratio within FFN blocks to match the target level of parameter reduction for fair comparison. More configuration details for pruning ratio and experimental settings are outlined in Appendix A.1. Best results in experiments are shaded as **first**, **second**, and **third**.

4.1. Large Language Models

QA Tasks. We report the QA performance comparisons with baselines in Table 2. Under a 20% pruning ratio, POP achieves the second-best performance across the majority of evaluated models. Under a 20% pruning ratio, POP outperforms Wanda-sp, FLAP, and Probe Pruning by 18.92%, 12.78%, and 1.05% on average, respectively. Although POP shows a modest performance gap of 1.38% relative to Týr, this difference can be attributed to Týr’s reliance on offline evolutionary search with calibration data. By contrast, POP performs pruning decisions entirely online.

Generation Tasks. We report the results on generation tasks in Table 2. Existing baselines, which rely on a static pruning mask during decoding, suffer from substantial performance degradation on generation tasks compared to QA settings. This degradation is particularly pronounced for long-form generation, where offline pruning methods like Wanda-sp and FLAP exhibit near-collapse even under moderate pruning ratios. In contrast, POP consistently outperforms all baseline methods across all evaluated models and pruning ratios. Under a 20% pruning ratio, POP achieves average performance improvements of 35.52%, 29.58%, 10.35%, and 12.51%, respectively, over the competing baselines. Moreover, the performance gap is markedly larger on generation tasks, underscoring the need for context-conditioned pruning during autoregressive decoding.

4.2. Mixture-of-Expert Models

We evaluate POP on MoE models using the same protocol as for dense LLMs. As shown in Table 3, POP consistently outperforms baselines across both QA and generation tasks under different pruning ratios. At a pruning ratio of

Table 2. Average results for Llama-2 (Touvron et al., 2023), Llama-3.1 (Dubey et al., 2024), and Qwen-3 (Yang et al., 2025a) across different pruning ratios on 7 QA tasks and 5 Generation tasks. The dash symbol indicates the corresponding setting is not applicable.

PR	Method	Online	Average QA tasks Accuracy (%) ↑								Average Generation tasks Accuracy (%) ↑							
			Llama2			Llama3.1		Qwen3		Avg.	Llama2			Llama3.1		Qwen3		Avg.
7B	13B	70B	8B	70B	8B	32B		7B	13B	70B	8B	70B	8B	32B		7B	13B	70B
0%	N/A	N/A	59.70	63.00	66.96	64.68	69.44	65.74	68.28	65.40	28.69	33.07	45.49	44.58	61.14	60.61	55.09	45.77
20%	Wanda-sp	✗	55.02	53.25	32.61	34.01	32.44	44.82	51.80	43.42	12.20	10.96	0.84	0.79	0.05	8.97	14.91	6.96
	FLAP	✗	54.24	57.87	35.34	53.02	38.55	54.44	53.50	49.56	17.23	19.04	2.99	16.48	1.68	14.91	17.97	12.90
	PP	✓	57.51	60.36	66.89	54.35	67.37	-	-	61.29	19.91	27.76	41.83	19.66	51.51	-	-	32.13
	Týr	✗	58.11	62.38	65.58	59.85	68.19	63.81	68.16	63.72	20.75	23.92	38.80	21.14	46.81	22.69	35.68	29.97
40%	Ours	✓	56.78	60.43	65.93	59.62	67.90	61.50	64.24	62.34	24.12	28.97	42.04	37.37	55.67	56.13	53.04	42.48
	Wanda-sp	✗	41.39	37.05	32.77	33.65	31.91	34.55	40.74	36.01	4.93	2.36	0.33	0.06	0.03	0.61	5.07	1.91
	FLAP	✗	45.65	47.59	33.00	43.17	34.41	36.66	40.75	40.17	9.08	14.19	0.19	6.84	0.64	0.40	6.08	5.35
	PP	✓	49.39	54.14	63.23	43.09	60.08	-	-	53.99	8.68	14.36	33.06	1.53	28.47	-	-	17.22
	Týr	✗	52.01	57.88	63.73	52.01	65.90	53.73	67.21	58.92	11.27	17.09	24.92	10.31	30.24	11.22	29.60	19.24
	Ours	✓	43.95	48.15	62.58	49.26	62.53	50.98	55.98	53.35	13.84	17.99	34.47	23.34	43.14	42.73	47.78	31.90

Table 3. Average results for Qwen1.5-MoE (Team, 2024), Qwen2-MoE (Yang et al., 2024) and Qwen3-MoE (Yang et al., 2025a) models across different pruning ratios on 7 QA tasks and 5 Generation tasks. The dash symbol indicates the corresponding setting is not applicable.

PR	Method	Avg. QA Acc. (%) ↑			Avg. Gen. Acc. (%) ↑		
		Q1.5 A2.7B	Q2 A14B	Q3 A3B	Q1.5 A2.7B	Q2 A14B	Q3 A3B
0%	N/A	60.21	64.71	66.76	43.17	54.92	57.77
20%	Wanda-sp	53.97	40.61	52.37	13.21	2.35	15.71
	FLAP	53.58	65.04	32.34	20.12	37.53	0.00
	Týr	59.61	-	63.80	27.66	-	43.07
	Ours	58.40	64.64	64.28	42.10	53.95	57.96
40%	Wanda-sp	38.04	34.43	39.01	2.71	0.39	1.54
	FLAP	49.81	58.12	32.34	15.15	17.26	0.00
	Týr	48.74	-	53.74	7.81	-	15.87
	Ours	53.95	64.24	54.94	31.11	53.86	38.65

Table 4. Average results for Qwen2-VL (Wang et al., 2024) and Qwen2.5-VL (Bai et al., 2025) on 5 VQA tasks under different pruning ratios.

PR	Qwen2-VL			Qwen2.5-VL		
	Wanda-sp	FLAP	Ours	Wanda-sp	FLAP	Ours
0%	-	-	62.14	-	-	60.68
20%	7.86	46.74	59.94	3.71	42.53	59.46
40%	0.02	0.01	54.33	0.00	0.00	54.63

20%, POP preserves strong QA performance while achieving substantially higher generation accuracy than baselines. Under a more aggressive 40% pruning ratio, baseline approaches exhibit severe degradation, whereas POP remains robust. These results suggest that online structural pruning is particularly beneficial for MoE architectures, possibly due to the additional variability introduced by dynamic expert routing between prefilling-stage importance estimation and decoding-stage computation.

Table 5. Comparison of inference latency between POP and Probe Pruning (Le et al., 2025) on Llama2-7B (Touvron et al., 2023). Latency is reported for attention, MLP, and end-to-end inference, with speedup measured relative to the dense model. Measurements are performed using CUDA event timing with input and output sequence lengths fixed to 128 tokens.

PR	Method	Attention		MLP		E2E Latency	
		Lat. (ms)	Speedup	Lat. (ms)	Speedup	Lat. (s)	Speedup
0%	Dense	42	-	53	-	3.04	-
20%	PP	40	1.05×	44	1.20×	2.69	1.13×
	Ours	42	1.00×	41	1.29×	2.66	1.14×
40%	PP	37	1.14×	30	1.77×	2.14	1.42×
	Ours	42	1.00×	27	1.96×	2.21	1.38×

4.3. Vision Language Models

We further evaluate the generalizability of POP on VLMs. We apply POP and baselines to Qwen2-VL and Qwen2.5-VL, and report their performance on five VQA benchmarks. As shown in Table 4, existing baselines suffer severe performance degradation under pruning, with accuracy dropping to near zero at higher sparsity levels. In contrast, POP consistently preserves strong VQA performance across both models. Under a 20% pruning ratio, POP achieves average improvements of 52.08% and 13.20% over Wanda-sp and FLAP on Qwen2-VL, and 55.75% and 16.93% on Qwen2.5-VL, respectively. These results demonstrate that POP generalizes effectively to multimodal architectures and remains robust across different application domains.

4.4. Inference Efficiency

To evaluate the efficiency of POP, we profile the latency of attention and FFN modules using CUDA event timing, and report the resulting end-to-end inference latency in Table 5. Since POP does not prune attention weights, attention latency remains unchanged, unlike Probe Pruning, which directly prunes attention weights. To achieve the same target

Table 6. Ablation study of the accuracy-efficiency trade-off under different pruning strategies. We report the mean accuracy over 5 generative tasks and the MLP-level FLOPs overhead. FLOPs are reported in TFLOPs, and overhead (%) denotes the relative increase in MLP computation compared to the dense FFN. Measurements are conducted using DeepSpeed (Rasley et al., 2020).

Model	Method	Mean	FLOPs	Overhead (%)
Llama2-7B	FFN	–	22.09	–
	Variant (1)	23.40	0.00	0.0
	Variant (2)	26.56	7.32	33.1
	Ours	24.12	0.63	2.85
Llama3.1-8B	FFN	–	28.75	–
	Variant (1)	34.69	0.00	0.0
	Variant (2)	38.95	9.56	33.3
	Ours	37.37	1.00	3.48

reduction in model parameters, POP applies a higher pruning ratio to the FFN layers. This design results in a more pronounced reduction in latency within the FFN blocks, partially compensating for the absence of attention pruning. As a result, POP achieves end-to-end inference latency comparable to Probe Pruning, while avoiding attention pruning during decoding. Overall, POP achieves inference speedups of $1.14\times$ and $1.38\times$ over the dense model under 20% and 40% pruning ratios, respectively.

5. Ablation Study

Accuracy–Efficiency Trade-off under Different Pruning Strategies. We justify the design of POP by comparing it with two alternative implementations that employ the same pruning metric and FFN-level structure.

As shown in Table 6, Variant (1) reuses the pruning mask obtained during the prefilling stage for all decoding steps. While this strategy introduces no additional overhead during decoding, the fixed pruning mask cannot adapt to the evolving decoding context, leading to a degradation in accuracy.

Variant (2) recomputes fine-grained pruning decisions over all channels at every decoding step. Although this approach achieves better performance, it incurs substantial computational overhead, introducing over 30% additional FFN FLOPs during decoding and largely offsetting the efficiency gains of structural pruning.

In contrast, POP achieves a more balanced trade-off. By restricting online pruning to a small candidate subset, it avoids full-channel re-evaluation and incurs less than 4% additional FFN cost with a partition fraction $\gamma = 0.1$, while consistently improving accuracy over Variant (1). These results demonstrate the effectiveness of POP in enabling efficient, context-conditioned online pruning.

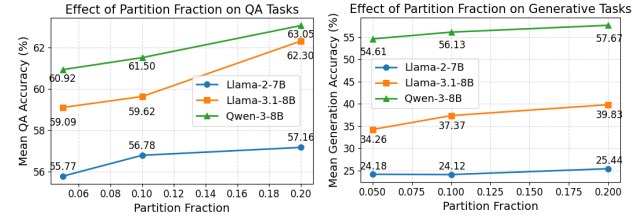


Figure 4. Ablation study on partition fraction γ in POP. Left: mean accuracy on zero-shot QA tasks. Right: mean accuracy on generative tasks.

Table 7. Comparison of offline preparation time (hours) for baseline pruning methods on Llama2-7B (Touvron et al., 2023), Llama3.1-70B (Dubey et al., 2024), and Qwen1.5-30B-A3B (Team, 2024). Zeros indicate that POP requires no offline preparation.

Model	Wanda-sp	FLAP	PP	Týr	POP
Llama2-7B	0.08	0.07	1.03	9.72	0.0
Llama3.1-70B	0.43	0.38	1.42	171.93	0.0
Qwen1.5-30B-A3B	1.14	0.85	–	45.44	0.0

Partition Fraction. To examine the effect of candidate region size, we vary the partition fraction γ in POP and evaluate its impact on both QA and generation tasks, as shown in Figure 4. As γ increases, the candidate region expands, allowing more channels to participate in online selection, which consistently improves accuracy across all evaluated models. However, a larger candidate region also incurs higher decoding-time computational overhead. Balancing performance and efficiency, we set $\gamma = 0.1$ as the default value in POP.

Offline Preparation Cost. Table 7 compares the offline preparation cost of different pruning methods. While Wanda-sp (Sun et al., 2024) and FLAP (An et al., 2024) incur minimal calibration overhead, Probe Pruning (Le et al., 2025) and Týr (Li et al., 2025) require substantial offline preprocessing, while Týr introduces the highest offline cost, exceeding one day of preprocessing on large-scale models like Llama3.1-70B with four default iterations. By contrast, POP is fully online and eliminates any offline preparation.

6. Conclusion

In this work, we propose POP, an efficient online structural pruning pipeline that overcomes the limitations of static pruning strategies by enabling context-conditioned online pruning with minimal overhead. Extensive experiments across LLMs, MoEs, and VLMs demonstrate that POP consistently outperforms SOTA pruning methods across nearly all evaluated settings. Beyond empirical improvements, POP highlights the importance of dynamic pruning decisions to evolving generation contexts, particularly during

autoregressive decoding. We hope this work inspires further exploration of contextual sparsity and online pruning mechanisms and contributes to the development of more efficient and adaptive inference techniques for LFM.

Impact Statement

This paper presents work whose goal is to advance the field of Machine Learning. There are many potential societal consequences of our work, none which we feel must be specifically highlighted here.

References

Akhauri, Y., AbouElhamayed, A. F., Dotzel, J., Zhang, Z., Rush, A. M., Huda, S., and Abdelfattah, M. S. Shadownllm: Predictor-based contextual sparsity for large language models. In *Proceedings of the 2024 Conference on Empirical Methods in Natural Language Processing*, pp. 19154–19167, 2024.

Alayrac, J.-B., Donahue, J., Luc, P., Miech, A., Barr, I., Hasson, Y., Lenc, K., Mensch, A., Millican, K., Reynolds, M., et al. Flamingo: a visual language model for few-shot learning. *Advances in neural information processing systems*, 35:23716–23736, 2022.

An, Y., Zhao, X., Yu, T., Tang, M., and Wang, J. Fluctuation-based adaptive structured pruning for large language models, 2023.

An, Y., Zhao, X., Yu, T., Tang, M., and Wang, J. Fluctuation-based adaptive structured pruning for large language models. In *Proceedings of the AAAI Conference on Artificial Intelligence*, volume 38, pp. 10865–10873, 2024.

Ashkboos, S., Croci, M. L., Nascimento, M. G. d., Hoefler, T., and Hensman, J. Slicept: Compress large language models by deleting rows and columns. In *International Conference on Learning Representations*, 2024.

Austin, J., Odena, A., Nye, M., Bosma, M., Michalewski, H., Dohan, D., Jiang, E., Cai, C., Terry, M., Le, Q., et al. Program synthesis with large language models. *arXiv preprint arXiv:2108.07732*, 2021.

Bai, S., Chen, K., Liu, X., Wang, J., Ge, W., Song, S., Dang, K., Wang, P., Wang, S., Tang, J., Zhong, H., Zhu, Y., Yang, M., Li, Z., Wan, J., Wang, P., Ding, W., Fu, Z., Xu, Y., Ye, J., Zhang, X., Xie, T., Cheng, Z., Zhang, H., Yang, Z., Xu, H., and Lin, J. Qwen2.5-vl technical report. *arXiv preprint arXiv:2502.13923*, 2025.

Bills, S., Cammarata, N., Mossing, D., Tillman, H., Gao, L., Goh, G., Sutskever, I., Leike, J., Wu, J., and Saunders, W. Language models can explain neurons in language models, 2023. URL <https://openaipublic.blob.core.windows.net/neuron-explainer/paper/index.html>.

Bommasani, R. On the opportunities and risks of foundation models. *arXiv preprint arXiv:2108.07258*, 2021.

Brown, T., Mann, B., Ryder, N., Subbiah, M., Kaplan, J. D., Dhariwal, P., Neelakantan, A., Shyam, P., Sastry, G., Askell, A., et al. Language models are few-shot learners. *Advances in neural information processing systems*, 33: 1877–1901, 2020.

Chen, M., Tworek, J., Jun, H., Yuan, Q., de Oliveira Pinto, H. P., Kaplan, J., Edwards, H., Burda, Y., Joseph, N., Brockman, G., Ray, A., Puri, R., Krueger, G., Petrov, M., Khlaaf, H., Sastry, G., Mishkin, P., Chan, B., Gray, S., Ryder, N., Pavlov, M., Power, A., Kaiser, L., Bavarian, M., Winter, C., Tillet, P., Such, F. P., Cummings, D., Plappert, M., Chantzis, F., Barnes, E., Herbert-Voss, A., Guss, W. H., Nichol, A., Paino, A., Tezak, N., Tang, J., Babuschkin, I., Balaji, S., Jain, S., Saunders, W., Hesse, C., Carr, A. N., Leike, J., Achiam, J., Misra, V., Morikawa, E., Radford, A., Knight, M., Brundage, M., Murati, M., Mayer, K., Welinder, P., McGrew, B., Amodei, D., McCandlish, S., Sutskever, I., and Zaremba, W. Evaluating large language models trained on code, 2021.

Chowdhery, A., Narang, S., Devlin, J., Bosma, M., Mishra, G., Roberts, A., Barham, P., Chung, H. W., Sutton, C., Gehrmann, S., et al. Palm: Scaling language modeling with pathways. *Journal of Machine Learning Research*, 24(240):1–113, 2023.

Clark, C., Lee, K., Chang, M.-W., Kwiatkowski, T., Collins, M., and Toutanova, K. BoolQ: Exploring the surprising difficulty of natural yes/no questions. In Burstein, J., Doran, C., and Solorio, T. (eds.), *Proceedings of the 2019 Conference of the North American Chapter of the Association for Computational Linguistics: Human Language Technologies, Volume 1 (Long and Short Papers)*, pp. 2924–2936, Minneapolis, Minnesota, June 2019. Association for Computational Linguistics. doi: 10.18653/v1/N19-1300. URL <https://aclanthology.org/N19-1300/>.

Clark, P., Cowhey, I., Etzioni, O., Khot, T., Sabharwal, A., Schoenick, C., and Tafjord, O. Think you have solved question answering? try arc, the ai2 reasoning challenge. *arXiv:1803.05457v1*, 2018.

Cobbe, K., Kosaraju, V., Bavarian, M., Chen, M., Jun, H., Kaiser, L., Plappert, M., Tworek, J., Hilton, J., Nakano, R., Hesse, C., and Schulman, J. Training verifiers to solve math word problems. *arXiv preprint arXiv:2110.14168*, 2021.

Denton, E. L., Zaremba, W., Bruna, J., LeCun, Y., and Fergus, R. Exploiting linear structure within convolutional networks for efficient evaluation. *Advances in neural information processing systems*, 27, 2014.

Dettmers, T., Lewis, M., Belkada, Y., and Zettlemoyer, L. Gpt3. int8 (): 8-bit matrix multiplication for transformers at scale. *Advances in neural information processing systems*, 35:30318–30332, 2022.

Dikkala, N., Ghosh, N., Meka, R., Panigrahy, R., Vyas, N., and Wang, X. On the benefits of learning to route in mixture-of-experts models. In *Proceedings of the 2023 Conference on Empirical Methods in Natural Language Processing*, pp. 9376–9396. Association for Computational Linguistics, 2023.

Du, N., Huang, Y., Dai, A. M., Tong, S., Lepikhin, D., Xu, Y., Krikun, M., Zhou, Y., Yu, A. W., Firat, O., et al. Glam: Efficient scaling of language models with mixture-of-experts. In *International conference on machine learning*, pp. 5547–5569. PMLR, 2022.

Dubey, A., Jauhri, A., Pandey, A., Kadian, A., Al-Dahle, A., Letman, A., Mathur, A., Schelten, A., Yang, A., Fan, A., et al. The llama 3 herd of models. *arXiv e-prints*, pp. arXiv–2407, 2024.

Fedus, W., Zoph, B., and Shazeer, N. Switch transformers: Scaling to trillion parameter models with simple and efficient sparsity. *Journal of Machine Learning Research*, 23(120):1–39, 2022.

Frantar, E. and Alistarh, D. Sparsegpt: Massive language models can be accurately pruned in one-shot. In *International Conference on Machine Learning*, pp. 10323–10337. PMLR, 2023.

Fu, C., Chen, P., Shen, Y., Qin, Y., Zhang, M., Lin, X., Yang, J., Zheng, X., Li, K., Sun, X., Wu, Y., Ji, R., Shan, C., and He, R. Mme: A comprehensive evaluation benchmark for multimodal large language models, 2025. URL <https://arxiv.org/abs/2306.13394>.

Gao, L., Tow, J., Abbasi, B., Biderman, S., Black, S., DiPofi, A., Foster, C., Golding, L., Hsu, J., Le Noac'h, A., Li, H., McDonell, K., Muennighoff, N., Ociepa, C., Phang, J., Reynolds, L., Schoelkopf, H., Skowron, A., Sutawika, L., Tang, E., Thite, A., Wang, B., Wang, K., and Zou, A. The language model evaluation harness, 07 2024. URL <https://zenodo.org/records/12608602>.

Geva, M., Schuster, R., Berant, J., and Levy, O. Transformer feed-forward layers are key-value memories. In *Proceedings of the 2021 Conference on Empirical Methods in Natural Language Processing*, pp. 5484–5495. Association for Computational Linguistics, 2021.

Gupta, A., Dollar, P., and Girshick, R. Lvis: A dataset for large vocabulary instance segmentation. In *Proceedings of the IEEE/CVF conference on computer vision and pattern recognition*, pp. 5356–5364, 2019.

Han, S., Mao, H., and Dally, W. J. Deep compression: Compressing deep neural networks with pruning, trained quantization and huffman coding. *arXiv preprint arXiv:1510.00149*, 2015a.

Han, S., Pool, J., Tran, J., and Dally, W. Learning both weights and connections for efficient neural network. *Advances in neural information processing systems*, 28, 2015b.

He, J. and Lin, H. Olica: Efficient structured pruning of large language models without retraining. In *International Conference on Machine Learning*. PMLR, 2025.

Hou, B., Chen, Q., Wang, J., Yin, G., Wang, C., Du, N., Pang, R., Chang, S., and Lei, T. Instruction-following pruning for large language models. In *International Conference on Machine Learning*. PMLR, 2025.

Hu, E. J., Shen, Y., Wallis, P., Allen-Zhu, Z., Li, Y., Wang, S., Wang, L., Chen, W., et al. Lora: Low-rank adaptation of large language models. In *International Conference on Learning Representations*, 2022.

Hu, H., Zhao, P., Li, P., Zheng, Y., Wang, Z., and Yuan, X. Fasp: Fast and accurate structured pruning of large language models. *arXiv preprint arXiv:2501.09412*, 2025.

Hudson, D. A. and Manning, C. D. Gqa: A new dataset for real-world visual reasoning and compositional question answering, 2019. URL <https://arxiv.org/abs/1902.09506>.

Jacob, B., Kligys, S., Chen, B., Zhu, M., Tang, M., Howard, A., Adam, H., and Kalenichenko, D. Quantization and training of neural networks for efficient integer-arithmetic-only inference. In *Proceedings of the IEEE conference on computer vision and pattern recognition*, pp. 2704–2713, 2018.

Kaplan, J., McCandlish, S., Henighan, T., Brown, T. B., Chess, B., Child, R., Gray, S., Radford, A., Wu, J., and Amodei, D. Scaling laws for neural language models. *arXiv preprint arXiv:2001.08361*, 2020.

Ke, L., Ye, M., Danelljan, M., Tai, Y.-W., Tang, C.-K., Yu, F., et al. Segment anything in high quality. *Advances in Neural Information Processing Systems*, 36:29914–29934, 2023.

Kirillov, A., Mintun, E., Ravi, N., Mao, H., Rolland, C., Gustafson, L., Xiao, T., Whitehead, S., Berg, A. C., Lo, W.-Y., et al. Segment anything. In *Proceedings of the*

IEEE/CVF international conference on computer vision, pp. 4015–4026, 2023.

Koike-Akino, T., Liu, J., and Wang, Y. mu-moe: Test-time pruning as micro-grained mixture-of-experts. *arXiv preprint arXiv:2505.18451*, 2025.

Kurtić, E., Frantar, E., and Alistarh, D. Ziplm: Inference-aware structured pruning of language models. *Advances in Neural Information Processing Systems*, 36:65597–65617, 2023.

Kwiatkowski, T., Palomaki, J., Redfield, O., Collins, M., Parikh, A., Alberti, C., Epstein, D., Polosukhin, I., Devlin, J., Lee, K., Toutanova, K., Jones, L., Kelcey, M., Chang, M.-W., Dai, A. M., Uszkoreit, J., Le, Q., and Petrov, S. Natural questions: A benchmark for question answering research. *Transactions of the Association for Computational Linguistics*, 7:453–466, 08 2019. ISSN 2307-387X. doi: 10.1162/tacl_a_00276. URL https://doi.org/10.1162/tacl_a_00276.

Le, Q., Diao, E., Wang, Z., Wang, X., Ding, J., Yang, L., and Anwar, A. Probe pruning: Accelerating llms through dynamic pruning via model-probing. In *International Conference on Learning Representations*, 2025.

Lee, D., Lee, J.-Y., Zhang, G., Tiwari, M., and Mirhoseini, A. Cats: Contextually-aware thresholding for sparsity in large language models. *Conference on Language Modeling*, 2024.

Lepikhin, D., Lee, H., Xu, Y., Chen, D., Firat, O., Huang, Y., Krikun, M., Shazeer, N., and Chen, Z. Gshard: Scaling giant models with conditional computation and automatic sharding. *International Conference on Learning Representations*, 2021.

Li, G., Xu, Y., Li, Z., Liu, J., Yin, X., Li, D., and Barsoum, E. Týr-the-pruner: Structural pruning llms via global sparsity distribution optimization. In *NeurIPS 2025*, 2025. URL <https://neurips.cc/virtual/2025/poster/115807>.

Li, Y., Mao, H., Girshick, R., and He, K. Exploring plain vision transformer backbones for object detection. In *European conference on computer vision*, pp. 280–296. Springer, 2022.

Li, Y., Du, Y., Zhou, K., Wang, J., Zhao, W. X., and Wen, J.-R. Evaluating object hallucination in large vision-language models. *arXiv preprint arXiv:2305.10355*, 2023.

Lin, T.-Y., Maire, M., Belongie, S., Hays, J., Perona, P., Ramanan, D., Dollár, P., and Zitnick, C. L. Microsoft coco: Common objects in context. In *European conference on computer vision*, pp. 740–755. Springer, 2014.

Liu, A., Feng, B., Xue, B., Wang, B., Wu, B., Lu, C., Zhao, C., Deng, C., Zhang, C., Ruan, C., et al. Deepseek-v3 technical report. *arXiv preprint arXiv:2412.19437*, 2024.

Liu, H., Tian, C., Wei, X., Dai, J., Liu, Q., Wei, T., Li, Q., and Li, L. Rap: Runtime-adaptive pruning for llm inference. *arXiv preprint arXiv:2505.17138*, 2025a.

Liu, J., Ponnusamy, P., Cai, T., Guo, H., Kim, Y., and Athiwaratkun, B. Training-free activation sparsity in large language models. In *International Conference on Learning Representations*, 2025b.

Liu, Z., Li, F., Li, G., and Cheng, J. Ebert: Efficient bert inference with dynamic structured pruning. In *Findings of the Association for Computational Linguistics*, pp. 4814–4823, 2021.

Liu, Z., Wang, J., Dao, T., Zhou, T., Yuan, B., Song, Z., Shrivastava, A., Zhang, C., Tian, Y., Re, C., et al. Deja vu: Contextual sparsity for efficient llms at inference time. In *International Conference on Machine Learning*, pp. 22137–22176. PMLR, 2023.

Lu, P., Mishra, S., Xia, T., Qiu, L., Chang, K.-W., Zhu, S.-C., Tafjord, O., Clark, P., and Kalyan, A. Learn to explain: Multimodal reasoning via thought chains for science question answering. In *The 36th Conference on Neural Information Processing Systems (NeurIPS)*, 2022.

Luo, X., Fu, X., Jiang, Z., and Zhou, S. K. Icp: Immediate compensation pruning for mid-to-high sparsity. In *Proceedings of the IEEE/CVF Conference on Computer Vision and Pattern Recognition*, pp. 9487–9496, June 2025.

Ma, X., Fang, G., and Wang, X. Llm-pruner: On the structural pruning of large language models. *Advances in Neural Information Processing Systems*, 36:21702–21720, 2023.

Marino, K., Rastegari, M., Farhadi, A., and Mottaghi, R. Ok-vqa: A visual question answering benchmark requiring external knowledge, 2019. URL <https://arxiv.org/abs/1906.00067>.

Men, X., Xu, M., Zhang, Q., Wang, B., Lin, H., Lu, Y., Han, X., and Chen, W. Shortgpt: Layers in large language models are more redundant than you expect, 2024. *Association for Computational Linguistics*, 2(3):4, 2024.

Merity, S., Xiong, C., Bradbury, J., and Socher, R. Pointer sentinel mixture models, 2016.

Michel, P., Levy, O., and Neubig, G. Are sixteen heads really better than one? *Advances in Neural Information Processing Systems*, 32, 2019.

Mihaylov, T., Clark, P., Khot, T., and Sabharwal, A. Can a suit of armor conduct electricity? a new dataset for open book question answering. In *EMNLP*, 2018.

Mirzadeh, I., Alizadeh, K., Mehta, S., Del Mundo, C. C., Tuzel, O., Samei, G., Rastegari, M., and Farajtabar, M. Relu strikes back: Exploiting activation sparsity in large language models. In *International Conference on Learning Representations*, 2024.

Patel, D., Gervacio, G., Raimi, D., Zhu, K., Lagasse, R., Grand, G., Panda, A., and Chaudhary, M. Alignment-constrained dynamic pruning for llms: Identifying and preserving alignment-critical circuits. *arXiv preprint arXiv:2511.07482*, 2025.

Penedo, G., Kydlíček, H., allal, L. B., Lozhkov, A., Mitchell, M., Raffel, C., Werra, L. V., and Wolf, T. The fineweb datasets: Decanting the web for the finest text data at scale. In *The Thirty-eight Conference on Neural Information Processing Systems Datasets and Benchmarks Track*, 2024. URL <https://openreview.net/forum?id=n6SCkn2QaG>.

Poliak, A. A survey on recognizing textual entailment as an nlp evaluation, 2020. URL <https://arxiv.org/abs/2010.03061>.

Radford, A., Kim, J. W., Hallacy, C., Ramesh, A., Goh, G., Agarwal, S., Sastry, G., Askell, A., Mishkin, P., Clark, J., et al. Learning transferable visual models from natural language supervision. In *International conference on machine learning*, pp. 8748–8763. PMLR, 2021.

Raffel, C., Shazeer, N., Roberts, A., Lee, K., Narang, S., Matena, M., Zhou, Y., Li, W., and Liu, P. J. Exploring the limits of transfer learning with a unified text-to-text transformer. *Journal of machine learning research*, 21(140):1–67, 2020.

Rasley, J., Rajbhandari, S., Ruwase, O., and He, Y. Deep-speed: System optimizations enable training deep learning models with over 100 billion parameters. In *Proceedings of the 26th ACM SIGKDD International Conference on Knowledge Discovery & Data Mining*, KDD ’20, pp. 3505–3506, New York, NY, USA, 2020. Association for Computing Machinery. ISBN 9781450379984. doi: 10.1145/3394486.3406703. URL <https://doi.org/10.1145/3394486.3406703>.

Reddy, S., Chen, D., and Manning, C. D. Coqa: A conversational question answering challenge, 2019. URL <https://arxiv.org/abs/1808.07042>.

Sakaguchi, K., Bras, R. L., Bhagavatula, C., and Choi, Y. Winogrande: An adversarial winograd schema challenge at scale, 2019. URL <https://arxiv.org/abs/1907.10641>.

Song, Y., Mi, Z., Xie, H., and Chen, H. Powerinfer: Fast large language model serving with a consumer-grade gpu. In *Proceedings of the ACM SIGOPS 30th Symposium on Operating Systems Principles*, pp. 590–606, 2024.

Sun, M., Liu, Z., Bair, A., and Kolter, J. Z. A simple and effective pruning approach for large language models. In *International Conference on Learning Representations*, 2024.

Team, Q. Qwen1.5-moe: Matching 7b model performance with 1/3 activated parameters”, February 2024. URL <https://qwenlm.github.io/blog/qwen-moe/>.

Touvron, H., Martin, L., Stone, K., Albert, P., Almahairi, A., Babaei, Y., Bashlykov, N., Batra, S., Bhargava, P., Bhosale, S., et al. Llama 2: Open foundation and fine-tuned chat models. *arXiv preprint arXiv:2307.09288*, 2023.

Wang, P., Bai, S., Tan, S., Wang, S., Fan, Z., Bai, J., Chen, K., Liu, X., Wang, J., Ge, W., Fan, Y., Dang, K., Du, M., Ren, X., Men, R., Liu, D., Zhou, C., Zhou, J., and Lin, J. Qwen2-vl: Enhancing vision-language model’s perception of the world at any resolution. *arXiv preprint arXiv:2409.12191*, 2024.

Wang, Z., Wohlwend, J., and Lei, T. Structured pruning of large language models. In Webber, B., Cohn, T., He, Y., and Liu, Y. (eds.), *Proceedings of the 2020 Conference on Empirical Methods in Natural Language Processing (EMNLP)*, pp. 6151–6162. Association for Computational Linguistics, 2020.

Xia, M., Zhong, Z., and Chen, D. Structured pruning learns compact and accurate models. In *Association for Computational Linguistics*, 2022.

Xia, M., Gao, T., Zeng, Z., and Chen, D. Sheared llama: Accelerating language model pre-training via structured pruning. In *International Conference on Learning Representations*, 2024.

Xu, P., Shao, W., Chen, M., Tang, S., Zhang, K., Gao, P., An, F., Qiao, Y., and Luo, P. Besa: Pruning large language models with blockwise parameter-efficient sparsity allocation. In *International Conference on Learning Representations*, 2024.

Yang, A., Yang, B., Hui, B., Zheng, B., Yu, B., Zhou, C., Li, C., Li, C., Liu, D., Huang, F., Dong, G., Wei, H., Lin, H., Tang, J., Wang, J., Yang, J., Tu, J., Zhang, J., Ma, J., Yang, J., Xu, J., Zhou, J., Bai, J., He, J., Lin, J., Dang, K., Lu, K., Chen, K., Yang, K., Li, M., Xue, M., Ni, N., Zhang, P., Wang, P., Peng, R., Men, R., Gao, R., Lin, R., Wang, S., Bai, S., Tan, S., Zhu, T., Li, T.,

Liu, T., Ge, W., Deng, X., Zhou, X., Ren, X., Zhang, X., Wei, X., Ren, X., Liu, X., Fan, Y., Yao, Y., Zhang, Y., Wan, Y., Chu, Y., Liu, Y., Cui, Z., Zhang, Z., Guo, Z., and Fan, Z. Qwen2 technical report, 2024. URL <https://arxiv.org/abs/2407.10671>.

Yang, A., Li, A., Yang, B., Zhang, B., Hui, B., Zheng, B., Yu, B., Gao, C., Huang, C., Lv, C., et al. Qwen3 technical report. *arXiv preprint arXiv:2505.09388*, 2025a.

Yang, M., Lin, S., Li, C., and Chang, X. Let llm tell what to prune and how much to prune. In *International Conference on Machine Learning*. PMLR, 2025b.

Yin, L., Wu, Y., Zhang, Z., Hsieh, C.-Y., Wang, Y., Jia, Y., Li, G., Jaiswal, A., Pechenizkiy, M., Liang, Y., et al. Outlier weighed layerwise sparsity (owl): A missing secret sauce for pruning llms to high sparsity. In *International Conference on Machine Learning*. PMLR, 2025.

Zellers, R., Holtzman, A., Bisk, Y., Farhadi, A., and Choi, Y. Hellaswag: Can a machine really finish your sentence? In *Proceedings of the 57th Annual Meeting of the Association for Computational Linguistics*, 2019.

Zhang, H., Li, F., Liu, S., Zhang, L., Su, H., Zhu, J., Ni, L. M., and Shum, H.-Y. Dino: Detr with improved denoising anchor boxes for end-to-end object detection. *arXiv preprint arXiv:2203.03605*, 2022.

Zhang, K., Li, B., Zhang, P., Pu, F., Cahyono, J. A., Hu, K., Liu, S., Zhang, Y., Yang, J., Li, C., and Liu, Z. Lmms-eval: Reality check on the evaluation of large multimodal models, 2024a. URL <https://arxiv.org/abs/2407.12772>.

Zhang, M., Chen, H., Shen, C., Yang, Z., Ou, L., Yu, X., and Zhuang, B. Loraprune: Structured pruning meets low-rank parameter-efficient fine-tuning. In *Findings of the Association for Computational Linguistics*, pp. 3013–3026. Association for Computational Linguistics, 2024b.

Zhang, Y., Li, Y., Wang, X., Shen, Q., Plank, B., Bischl, B., Rezaei, M., and Kawaguchi, K. Finercut: finer-grained interpretable layer pruning for large language models. *arXiv preprint arXiv:2405.18218*, 2024c.

Zhong, L., Wan, F., Chen, R., Quan, X., and Li, L. Block-pruner: Fine-grained pruning for large language models. In *Findings of the Association for Computational Linguistics: ACL 2025*, pp. 5065–5080, 2025.

Zhou, Y., Lei, T., Liu, H., Du, N., Huang, Y., Zhao, V., Dai, A. M., Le, Q. V., Laudon, J., et al. Mixture-of-experts with expert choice routing. *Advances in Neural Information Processing Systems*, 35:7103–7114, 2022.

Zhou, Y., Chen, Z., Xu, Z., Lin, X. V., and Chen, B. Sirius: Contextual sparsity with correction for efficient llms. *Advances in Neural Information Processing Systems*, 37: 24046–24080, 2024.

A. Implementation Details

In this section, we provide a detailed description of the experimental methodologies employed for both POP and the baseline approaches. We elaborate on the specific configurations and implementation settings to ensure a rigorous and fair evaluation.

A.1. Pruning Ratio Configurations

For the baseline methods Wanda-sp (Sun et al., 2024) and Probe Pruning (Le et al., 2025), a uniform pruning ratio is applied to both the self-attention and MLP layers, identical to the overall target sparsity. In contrast, FLAP (An et al., 2023), which aggregates scores across all components, and Týr (Li et al., 2025), which utilizes evolutionary search, dynamically allocate pruning ratios between attention and MLP layers while satisfying the global target pruning ratio.

To ensure robust performance in generative tasks, POP exclusively conducts MLP weight pruning and preserves attention mechanisms. We adjust the pruning ratio within the MLP blocks to match the total parameter reduction of these baselines for a fair comparison. Consequently, the effective sparsity applied to MLPs is inherently higher than the overall target pruning ratio. The specific effective MLP pruning ratios corresponding to each target FLOPs reduction are detailed in Table 8. All experiments were conducted on NVIDIA A6000 clusters.

Table 8. Proper MLP pruning ratios required to achieve the target FLOPs reduction. Since our method preserves attention layers, we apply higher sparsity to MLP blocks compared to the target pruning ratio. All values are rounded to the first decimal place.

Target PR	MLP Pruning Ratio (%)									
	LLM					MoE			VLM	
	Llama2		Llama3.1		Qwen3	Qwen1.5	Qwen2	Qwen3	Qwen2	Qwen2.5
	7B	13B	70B	8B	70B	8B	32B	A2.7B	57B-A14B	30B-A3B
20%	29.9	29.9	24.3	24.8	24.3	25.6	24.8	29.7	22.7	30.0
40%	59.8	59.8	48.6	49.5	48.6	51.1	49.6	59.4	45.3	60.0
									22.9	22.9
									45.8	45.8

A.2. Offline Calibration Stage

To ensure a fair comparison, we utilized the C4 dataset (Raffel et al., 2020) with 2,000 samples for Wanda-sp (Sun et al., 2024), FLAP (An et al., 2023), and Probe Pruning (Le et al., 2025). However, we distinguished the sequence length settings based on methodological requirements. For Wanda-sp and FLAP, we set the sequence length to 1,024 tokens. In contrast, for Probe Pruning, we employed a sequence length of 4,096 tokens. This setting matches the maximum position embedding of Llama2 and was necessary because Probe Pruning requires a historical state longer than the input sequence length to support generative tasks.

For Týr (Li et al., 2025), we adhered to the configuration specified in the original literature. We used the FineWeb dataset (Penedo et al., 2024) for calibration, conducting the offline stage with 1,000 samples and a maximum input length of 4k tokens. Finally, POP operates exclusively via online pruning, eliminating the need for a separate offline calibration stage.

A.3. Perplexity

Table 9 presents the perplexity scores on the WikiText (Merity et al., 2016) benchmark. The primary goal of this experiment is to evaluate the robustness of the compressed models in general language understanding and generation scenarios. While accuracy metrics on QA tasks demonstrate task-specific proficiency, perplexity provides a complementary view of the model’s stability by quantifying the uncertainty in token prediction. A lower perplexity indicates that the pruned model maintains a probability distribution close to that of the dense model.

A.4. Evaluation Metrics

Table 10 presents the evaluation metrics for the tasks used in the experiments. For LLM QA tasks, we consistently used Accuracy as the primary metric. In the case of LLM Generation tasks, we employed F1 Score for CoQA, Pass@1 for MBPP and HumanEval, and Exact Match for NQ Open and GSM8K. For VLM tasks, we utilized F1 Score for POPE, Exact Match for OK-VQA, GQA, and ScienceQA, and Perception Score for MME. To calculate the mean value for each category, we standardized all metrics to a 100-point scale. Since Accuracy, F1 Score, Pass@1, and Exact Match have a maximum value of 1, they were converted to percentages. For MME, which uses Perception Score, we normalized the score based on the

Table 9. Wikitext (Merity et al., 2016) perplexity results for LLM and MoE models across different pruning ratios. Lower perplexity (\downarrow) indicates better performance. Experiments are conducted using a batch size 10.

PR	Method	Online	Wikitext Perplexity (LLMs) \downarrow					Wikitext Perplexity (MoEs) \downarrow	
			Llama2			Qwen3		Qwen1.5-MoE	Qwen2
			7B	13B	70B	8B	32B	A2.7B	57B-A14B
0%	N/A	N/A	5.12	4.57	3.12	9.00	7.02	6.79	5.56
20%	Wanda-sp	✗	9.23	7.90	466.51	785.16	11.55	9.92	58.76
	FLAP	✗	7.53	6.64	123.74	13.99	8.23	9.64	6.02
	PP	✓	6.17	5.25	3.61	-	-	-	-
	Týr	✗	6.44	5.41	4.25	11.66	7.20	7.73	-
40%	Ours	✓	6.86	5.94	3.92	10.95	8.44	7.51	5.75
	Wanda-sp	✗	23.26	50.55	629.09	868.30	33.72	75.00	822.18
	FLAP	✗	20.06	11.48	505.42	157.43	24.37	16.53	58.76
	PP	✓	9.82	7.34	4.62	-	-	-	-
	Týr	✗	12.55	10.38	5.64	27.47	9.22	44.72	-
	Ours	✓	20.57	17.97	5.63	18.40	12.46	10.43	6.21

total possible score corresponding to the dataset size. Finally, we computed the macro average of these normalized scores to derive the mean value for each category.

Table 10. Evaluation Metrics and Tasks used in Experiments

Category	Task	Metric
LLM QA Tasks	BoolQ	Accuracy
	RTE	Accuracy
	HellaSwag	Accuracy
	Winogrande	Accuracy
	ARC-Easy	Accuracy
	ARC-Challenge	Accuracy
	OpenBookQA	Accuracy
LLM Generation Tasks	CoQA	F1 Score
	MBPP	Pass@1
	NQ Open	Exact Match
	HumanEval	Pass@1
	GSM8K	Exact Match
Language Modeling	WikiText	Perplexity
VLM Tasks	POPE	F1 Score
	OK-VQA	Exact Match
	GQA	Exact Match
	ScienceQA	Exact Match
	MME	Perception Score

B. Segment Anything Model

The Segment Anything Model (SAM) (Kirillov et al., 2023) comprises a heavy image encoder, a prompt encoder, and a lightweight mask decoder. Notably, the image encoder accounts for over 90% of the parameters and dominates inference costs, making it a prime candidate for pruning-based acceleration. To validate the extensibility of POP to this pure vision architecture, we adapted our method to target the image encoder. Unlike autoregressive models that utilize a token decoding loop, SAM operates via a single-pass representation; consequently, we applied POP exclusively using the strategy designed for the *prefilling phase*. Given the lack of established structured pruning baselines for this architecture, we implemented a **Random structured pruning** baseline for comparison.

Table 11. Detailed Accuracies (%) on COCO dataset (Lin et al., 2014) using SAM models with different levels of structured sparsity. We compare the dense model with POP and Random structured pruning at 20% sparsity. For the COCO dataset, we use a SOTA detector FocalNet-DINO (Zhang et al., 2022) trained on the COCO dataset as our box prompt generator. Bold indicates the better performance between POP and Random.

Model	Method	PR (%)	AP	AP ₅₀	AP ₇₅	AP _s	AP _m	AP _l	AP _{avg}
ViT-B	Dense	–	46.16	73.17	49.21	34.61	50.52	59.32	52.16
	Random	20	44.31	71.76	46.36	32.02	48.66	57.86	50.16
	POP (Ours)	20	45.38	72.79	47.94	34.06	49.57	58.32	51.34
ViT-L	Dense	–	48.72	74.97	52.94	36.85	53.47	61.90	54.81
	Random	20	47.18	73.66	50.70	35.01	51.96	60.55	53.18
	POP (Ours)	20	47.23	74.14	50.68	35.88	51.71	59.93	53.26
ViT-H	Dense	–	49.03	75.20	53.23	37.13	54.14	61.78	55.09
	Random	20	47.70	73.98	51.68	35.52	52.82	61.25	53.82
	POP (Ours)	20	47.56	74.23	50.99	36.09	52.08	60.32	53.54

We evaluated zero-shot segmentation performance on the full validation sets to ensure statistical significance: 5,000 images for COCO (Lin et al., 2014) and 19,809 for LVIS (Gupta et al., 2019). All experiments were conducted with a batch size of 10. To generate box prompts, we adopted the **generators employed in HQ-SAM** (Ke et al., 2023): FocalNet-DINO (Zhang et al., 2022) for COCO and ViTDet-H (Li et al., 2022) for LVIS. The detailed experimental results are presented in Tables 11 and 12. These results demonstrate that POP effectively maintains performance compared to dense and random baselines, confirming its efficacy in pure vision architectures.

C. Additional Experimental Results

In this section, we present detailed experimental results stratified by task. Our evaluation encompasses dense models, POP models, and various baseline methods.

Tables 13, 14, 15, and 19 report the performance on zero-shot commonsense question-answering (QA) benchmarks for Large Language Models (LLMs) and Mixture-of-Experts (MoE) models. For text generation tasks, the results across LLMs and MoE models are provided in Tables 16, 17, 18, and 20. We also evaluate the language modeling capability of the models.

Moreover, Table 21 illustrates the experimental outcomes for Visual Question Answering (VQA) tasks using Vision-Language Models (VLMs).

Finally, Tables 22, 23, and 24 present the detailed results corresponding to the ablation study discussed in Section 5. Table 22 compares the performance of models under different pruning strategies. Tables 23 and 24 demonstrate the impact of the partition fraction, which is a hyperparameter of POP, on model accuracy for QA tasks and generative tasks, respectively.

Table 12. Detailed Accuracies (%) on LVIS dataset (Gupta et al., 2019) using SAM models with different levels of structured sparsity. We compare the dense model with POP and Random structured pruning at 20% sparsity. For LVIS, we adopt ViTDet-H (Li et al., 2022) trained on the LVIS dataset as our box prompt generator. Bold indicates the better performance between POP and Random.

Model	Method	PR (%)	AP	AP ₅₀	AP ₇₅	AP _s	AP _m	AP _l	AP _r	AP _c	AP _f	AP _{avg}
ViT-B	Dense	–	41.41	59.61	43.68	29.47	53.49	61.39	32.96	42.27	44.18	45.38
	Random	20	39.20	58.00	40.90	27.61	50.65	59.10	31.05	40.50	41.34	43.15
	POP (Ours)	20	41.07	59.28	43.51	29.56	52.87	60.49	32.60	41.99	43.76	45.02
ViT-L	Dense	–	44.01	60.78	46.63	31.48	56.77	65.46	33.84	44.94	47.44	47.93
	Random	20	42.26	59.72	44.56	29.70	54.79	64.15	32.75	43.31	45.26	46.28
	POP (Ours)	20	43.34	60.58	46.03	31.83	55.43	63.01	33.87	44.20	46.54	47.20
ViT-H	Dense	–	44.65	61.15	47.38	32.09	57.54	65.68	34.61	45.43	48.19	48.53
	Random	20	42.82	60.06	45.37	30.23	55.26	64.07	34.10	43.55	45.86	46.81
	POP (Ours)	20	43.66	60.68	46.37	31.76	55.77	63.87	34.14	44.31	47.13	47.52

Table 13. Detailed Accuracies (%) of Llama-2 (Touvron et al., 2023) for 7 QA tasks with different levels of structured sparsity.

Params	Method	PR(%)	BoolQ	RTE	HS	WG	ARC-e	ARC-c	OBQA	Mean
Llama2-7B	Dense	-	77.71	62.82	57.17	69.14	76.26	43.43	31.40	59.7
	Wanda-sp	20	68.53	53.79	54.74	67.25	72.18	39.85	28.80	55.02
	FLAP	20	68.90	61.01	51.89	66.06	66.50	36.35	29.00	54.24
	Probe Pruning	20	72.51	61.01	54.75	66.61	73.99	42.07	31.60	57.51
	Týr	20	75.60	62.46	53.94	68.35	74.71	41.30	30.40	58.11
	POP (Ours)	20	72.63	63.54	53.42	67.72	71.13	39.59	29.40	56.78
	Wanda-sp	40	61.74	54.51	35.08	51.14	49.37	23.12	14.80	41.39
	FLAP	40	63.39	50.54	42.92	62.59	49.03	27.05	24.00	45.65
	Probe Pruning	40	64.43	45.85	46.68	58.72	66.25	34.98	28.80	49.39
	Týr	40	69.27	49.46	46.44	64.01	68.98	37.12	28.80	52.01
Llama2-13B	POP (Ours)	40	64.04	50.18	37.71	57.46	50.76	27.73	19.80	43.95
	Dense	-	80.55	65.34	60.05	72.14	79.42	48.29	35.20	63
	Wanda-sp	20	67.46	54.15	48.56	67.48	69.74	37.54	27.80	53.25
	FLAP	20	73.49	60.65	55.98	71.90	71.13	42.15	29.80	57.87
	Probe Pruning	20	78.78	59.21	58.45	70.32	77.32	44.63	33.80	60.36
	Týr	20	79.82	68.59	58.01	73.01	77.65	46.16	33.40	62.38
	POP (Ours)	20	79.94	67.87	57.68	69.61	74.29	43.00	30.60	60.43
	Wanda-sp	40	62.17	52.71	30.07	51.46	31.52	20.05	11.40	37.05
	FLAP	40	63.43	53.07	42.00	61.64	55.14	31.06	26.80	47.59
	Probe Pruning	40	70.40	49.82	52.77	62.51	71.25	40.44	31.80	54.14
Llama2-70B	Týr	40	76.91	61.37	53.03	68.82	73.86	40.36	30.80	57.88
	POP (Ours)	40	68.23	56.32	42.32	60.62	55.51	32.42	21.60	48.15
	Dense	-	83.76	67.87	64.78	77.98	82.70	54.44	37.20	66.96
	Wanda-sp	20	37.83	51.99	26.84	49.49	29.42	19.71	13.00	32.61
	FLAP	20	50.55	49.46	30.01	48.38	34.55	20.05	14.40	35.34
	Probe Pruning	20	82.26	69.68	64.04	78.14	82.41	55.29	36.40	66.89
	Týr	20	77.10	69.68	63.80	75.85	81.31	54.35	37.00	65.58
	POP (Ours)	20	82.94	66.07	63.92	76.48	81.69	54.18	36.20	65.93
	Wanda-sp	40	38.23	54.87	26.24	49.80	27.23	21.42	11.60	32.77
	FLAP	40	39.63	54.87	26.49	49.80	26.05	20.99	13.20	33
	Probe Pruning	40	80.58	63.90	61.42	72.77	78.70	51.62	33.60	63.23
	Týr	40	76.15	69.31	60.63	76.56	78.49	49.15	35.80	63.73
	POP (Ours)	40	82.60	64.98	60.31	73.72	77.74	46.08	32.60	62.58

Table 14. Detailed Accuracies (%) of Llama-3 (Dubey et al., 2024) for 7 QA tasks with different levels of structured sparsity.

Params	Method	PR(%)	BoolQ	RTE	HS	WG	ARC-e	ARC-c	OBQA	Mean
Llama3.1-8B	Dense	-	81.96	70.76	60.01	73.72	81.48	51.45	33.40	64.68
	Wanda-sp	20	46.12	54.15	26.62	49.41	29.29	19.11	13.40	34.01
	FLAP	20	68.62	61.37	48.26	68.27	65.15	32.85	26.60	53.02
	Probe Pruning	20	67.92	53.79	53.02	63.30	73.36	40.44	28.60	54.35
	Týr	20	78.20	65.34	54.31	68.43	76.18	44.71	31.80	59.85
	POP (Ours)	20	77.28	63.90	54.68	70.88	76.22	44.20	30.20	59.62
	Wanda-sp	40	45.75	50.54	25.63	49.96	28.20	20.65	14.80	33.65
	FLAP	40	62.05	57.76	37.35	58.41	44.91	20.90	20.80	43.17
	Probe Pruning	40	58.62	53.07	33.78	54.85	55.98	25.51	19.80	43.09
	Týr	40	71.35	59.93	44.27	61.80	68.01	33.11	25.60	52.01
Llama3.1-70B	POP (Ours)	40	66.30	56.68	40.44	62.75	61.95	35.07	21.60	49.26
	Dense	-	85.38	69.68	66.43	79.24	87.21	60.92	37.20	69.44
	Wanda-sp	20	38.59	51.99	25.88	51.14	25.46	20.22	13.80	32.44
	FLAP	20	57.03	53.07	29.53	53.67	36.28	19.88	20.40	38.55
	Probe Pruning	20	85.60	66.07	63.82	78.30	84.72	58.28	34.80	67.37
	Týr	20	85.72	69.31	64.67	79.16	85.10	58.36	35.00	68.19
	POP (Ours)	20	84.25	68.95	65.32	78.14	85.86	58.36	34.40	67.9
	Wanda-sp	40	37.86	53.79	26.00	47.51	24.66	21.93	11.60	31.91
	FLAP	40	44.92	52.71	27.93	49.57	31.73	18.60	15.40	34.41
	Probe Pruning	40	77.98	62.46	57.10	70.48	78.24	45.48	28.80	60.08
	Týr	40	84.07	70.76	60.64	77.03	81.48	53.75	33.60	65.9
	POP (Ours)	40	78.78	67.15	58.81	72.46	80.09	50.85	29.60	62.53

Table 15. Detailed Accuracies (%) of Qwen3 (Yang et al., 2025a) for 7 QA tasks with different levels of structured sparsity.

Params	Method	PR(%)	BoolQ	RTE	HS	WG	ARC-e	ARC-c	OBQA	Mean
Qwen3-8B	Dense	-	86.61	77.98	57.10	68.11	83.29	55.46	31.60	65.74
	Wanda-sp	20	64.59	53.07	37.64	52.57	54.46	26.62	24.80	44.82
	FLAP	20	77.52	66.07	50.05	62.90	64.39	35.32	24.80	54.44
	Týr	20	84.62	74.73	54.27	67.56	81.61	52.47	31.40	63.81
	POP (Ours)	20	84.77	74.37	51.76	64.80	77.78	48.21	28.80	61.5
	Wanda-sp	40	48.41	48.74	27.65	50.20	34.39	18.86	13.60	34.55
	FLAP	40	57.62	51.63	32.31	51.07	32.28	19.54	12.20	36.66
	Týr	40	62.39	67.15	42.98	59.35	73.70	39.51	31.00	53.73
	POP (Ours)	40	76.67	65.70	39.52	57.14	60.31	32.34	25.20	50.98
	Dense	-	86.30	76.17	63.91	73.32	84.43	57.86	36.00	68.28
Qwen3-32B	Wanda-sp	20	72.39	59.57	49.21	59.12	63.47	36.86	22.00	51.8
	FLAP	20	85.96	79.06	61.13	67.40	25.08	22.70	33.20	53.5
	Týr	20	86.97	78.34	63.94	71.90	83.38	57.00	35.60	68.16
	POP (Ours)	20	85.72	76.53	60.94	65.43	76.85	52.22	32.00	64.24
	Wanda-sp	40	59.51	51.26	36.80	51.54	42.72	25.34	18.00	40.74
	FLAP	40	58.10	53.79	39.37	51.22	42.76	23.04	17.00	40.75
	Týr	40	85.75	75.45	61.08	70.64	83.71	57.85	36.00	67.21
	POP (Ours)	40	80.67	70.40	51.23	58.33	64.52	40.10	26.60	55.98

Table 16. Accuracies (%) of Llama-2 (Touvron et al., 2023) for 5 Generative tasks with different levels of structured sparsity.

Params	Method	PR	coqa	mbpp	nq-open	humaneval	gsm8k	Mean
Llama2-7B	Dense	-	77.35	23.40	18.89	9.76	14.03	28.69
	Wanda-sp	20	51.37	0.00	7.56	0.00	2.05	12.2
	FLAP	20	73.77	2.00	6.21	1.22	2.96	17.23
	Probe Pruning	20	66.46	8.40	10.80	6.71	7.20	19.91
	Týr	20	75.46	8.20	11.27	1.83	6.98	20.75
	POP (Ours)	20	76.46	16.20	9.78	7.93	10.24	24.12
	Wanda-sp	40	22.45	0.00	0.28	0.00	1.90	4.93
	FLAP	40	43.07	0.00	0.42	0.00	1.90	9.08
	Probe Pruning	40	38.18	1.40	2.38	0.00	1.44	8.68
	Týr	40	51.69	0.00	4.64	0.00	0.00	11.27
	POP (Ours)	40	56.44	3.80	2.02	3.05	3.87	13.84
Llama2-13B	Dense	-	79.18	27.20	23.63	12.20	23.12	33.07
	Wanda-sp	20	49.96	0.60	1.66	0.00	2.58	10.96
	FLAP	20	76.94	3.40	6.54	0.61	7.73	19.04
	Probe Pruning	20	76.05	20.80	15.43	10.37	16.15	27.76
	Týr	20	78.05	11.40	11.63	1.83	16.68	23.92
	POP (Ours)	20	79.00	21.60	13.85	9.76	20.62	28.97
	Wanda-sp	40	10.65	0.00	0.00	0.00	1.14	2.36
	FLAP	40	68.49	0.00	1.11	0.00	1.36	14.19
	Probe Pruning	40	52.36	5.20	5.18	3.66	5.38	14.36
	Týr	40	74.79	2.00	5.15	0.00	3.49	17.09
	POP (Ours)	40	59.51	10.00	2.91	6.10	11.45	17.99
Llama2-70B	Dense	-	83.71	45.00	29.00	16.46	53.30	45.49
	Wanda-sp	20	2.68	0.00	0.00	0.00	1.52	0.84
	FLAP	20	14.13	0.00	0.00	0.00	0.83	2.99
	Probe Pruning	20	82.24	39.00	23.30	14.02	50.57	41.83
	Týr	20	81.66	30.20	24.32	10.98	46.85	38.8
	POP (Ours)	20	83.09	38.00	23.82	14.63	50.64	42.04
	Wanda-sp	40	0.99	0.00	0.00	0.00	0.68	0.33
	FLAP	40	0.67	0.00	0.00	0.00	0.30	0.19
	Probe Pruning	40	79.98	25.60	14.07	10.98	34.65	33.06
	Týr	40	75.85	0.00	13.24	5.49	30.02	24.92
	POP (Ours)	40	81.71	24.00	11.52	14.02	41.09	34.47

Table 17. Accuracies (%) of Llama-3 (Dubey et al., 2024) for 5 Generative tasks with different levels of structured sparsity.

Params	Method	PR	coqa	mbpp	nq_open	humaneval	gsm8k	Mean
Llama3.1-8B	Dense	-	80.88	48.40	7.70	35.37	50.57	44.58
	Wanda-sp	20	3.12	0.00	0.00	0.00	0.83	0.79
	FLAP	20	73.01	1.80	2.83	1.22	3.56	16.48
	Probe Pruning	20	54.45	17.60	8.20	11.59	6.44	19.66
	Týr	20	75.52	8.60	4.85	7.93	8.79	21.14
	POP (Ours)	20	79.70	39.20	3.82	23.78	40.33	37.37
	Wanda-sp	40	0.00	0.00	0.06	0.00	0.23	0.06
	FLAP	40	32.16	0.00	0.00	0.00	2.05	6.84
	Probe Pruning	40	5.38	0.00	0.30	0.61	1.36	1.53
	Týr	40	45.51	0.00	4.15	0.00	1.90	10.31
	POP (Ours)	40	69.20	14.40	2.63	12.20	18.27	23.34
Llama3.1-70B	Dense	-	83.70	64.60	24.96	51.22	81.20	61.14
	Wanda-sp	20	0.19	0.00	0.06	0.00	0.00	0.05
	FLAP	20	7.04	0.00	0.06	0.00	1.29	1.68
	Probe Pruning	20	81.27	54.60	20.19	26.83	74.68	51.51
	Týr	20	82.51	47.20	20.64	15.85	67.85	46.81
	POP (Ours)	20	83.11	59.20	17.40	40.85	77.79	55.67
	Wanda-sp	40	0.07	0.00	0.00	0.00	0.08	0.03
	FLAP	40	2.58	0.00	0.03	0.00	0.61	0.64
	Probe Pruning	40	68.80	25.40	9.36	7.93	30.86	28.47
	Týr	40	78.85	15.40	8.25	5.49	43.22	30.24
	POP (Ours)	40	80.24	40.60	10.25	25.00	59.59	43.14

Table 18. Accuracies (%) of Qwen3 (Yang et al., 2025a) for 5 Generative tasks with different levels of structured sparsity.

Params	Method	PR	coqa	mbpp	nq_open	humaneval	gsm8k	Mean
Qwen3-8B	Dense	-	81.97	65.60	7.31	60.98	87.19	60.61
	Wanda-sp	20	43.16	0.00	0.11	0.00	1.59	8.97
	FLAP	20	72.11	0.00	0.55	0.00	1.90	14.91
	Týr	20	75.17	3.20	3.32	0.61	31.16	22.69
	POP (Ours)	20	81.05	56.00	2.35	56.10	85.14	56.13
	Wanda-sp	40	1.71	0.00	0.00	0.00	1.36	0.61
	FLAP	40	1.64	0.00	0.14	0.00	0.23	0.4
	Týr	40	48.71	0.00	5.32	0.00	2.05	11.22
	POP (Ours)	40	73.73	31.80	0.89	35.37	71.87	42.73
	Dense	-	82.45	78.20	2.52	37.81	74.45	55.09
Qwen3-32B	Wanda-sp	20	63.39	0.20	1.11	0.61	9.25	14.91
	FLAP	20	81.01	3.40	3.63	1.83	0.00	17.97
	Týr	20	81.31	44.00	1.14	0.00	51.93	35.68
	POP (Ours)	20	80.75	70.00	3.16	39.63	71.65	53.04
	Wanda-sp	40	24.21	0.00	0.08	0.00	1.06	5.07
	FLAP	40	29.31	0.00	0.03	0.00	1.06	6.08
	Týr	40	79.55	0.00	2.69	1.22	64.52	29.6
	POP (Ours)	40	75.98	49.20	1.63	37.81	74.30	47.78

Table 19. Detailed Accuracies (%) of Qwen1.5-MoE (Team, 2024), Qwen2-MoE (Yang et al., 2024) and Qwen3-MoE (Yang et al., 2025a) models for 7 QA tasks with different levels of structured sparsity.

Params	Method	PR(%)	BoolQ	RTE	HS	WG	ARC-e	ARC-c	OBQA	Mean
Qwen1.5-MoE A2.7B	Dense	-	79.73	68.59	57.98	69.53	73.06	41.81	30.80	60.21
	Wanda-sp	20	68.32	59.93	52.99	58.64	72.35	39.93	25.60	53.97
	FLAP	20	72.66	64.62	47.43	67.32	63.68	32.17	27.20	53.58
	Týr	20	76.64	69.31	53.56	69.77	74.96	41.81	31.20	59.61
	POP (Ours)	20	77.65	68.95	55.67	68.04	70.96	39.16	28.40	58.4
	Wanda-sp	40	62.17	52.71	29.56	53.20	36.79	19.28	12.60	38.04
	FLAP	40	64.04	62.09	42.89	64.17	59.85	30.46	25.20	49.81
	Týr	40	64.45	53.43	36.34	56.28	70.71	35.58	24.40	48.74
	POP (Ours)	40	74.89	62.09	47.21	66.69	66.50	35.24	25.00	53.95
Qwen2 57B-A14B	Dense	-	86.36	75.09	62.93	74.03	75.08	46.67	32.80	64.71
	Wanda-sp	20	59.17	53.07	32.63	53.51	46.97	23.55	15.40	40.61
	FLAP	20	87.25	75.45	62.78	75.14	76.60	46.08	32.00	65.04
	POP (Ours)	20	87.00	75.45	62.37	73.95	74.75	47.18	31.80	64.64
	Wanda-sp	40	48.20	52.71	27.15	49.65	27.19	21.93	14.20	34.43
	FLAP	40	73.73	67.51	55.80	68.27	70.92	41.38	29.20	58.12
	POP (Ours)	40	85.60	75.09	60.28	74.67	75.30	47.53	31.20	64.24
Qwen3 30B-A3B	Dense	-	88.75	82.31	59.56	70.56	79.29	52.82	34.00	66.76
	Wanda-sp	20	73.30	63.54	44.73	60.62	62.21	37.37	24.80	52.37
	FLAP	20	37.83	47.29	25.59	50.12	24.33	21.42	19.80	32.34
	Týr	20	86.33	77.26	53.10	68.90	77.36	48.04	35.60	63.8
	POP (Ours)	20	87.28	81.59	55.00	68.43	75.25	48.04	34.40	64.28
	Wanda-sp	40	56.70	50.18	34.49	49.49	41.71	23.72	16.80	39.01
	FLAP	40	37.83	47.29	25.59	50.12	24.33	21.42	19.80	32.34
	Týr	40	65.26	60.29	43.03	61.48	73.78	41.72	30.60	53.74
	POP (Ours)	40	79.63	74.73	41.72	63.54	63.13	36.43	25.40	54.94

Table 20. Detailed Accuracies (%) of Qwen1.5-MoE (Team, 2024), Qwen2-MoE (Yang et al., 2024) and Qwen3-MoE (Yang et al., 2025a) models for 5 Generative tasks with different levels of structured sparsity.

Params	Method	PR	coqa	mbpp	nq-open	humaneval	gsm8k	Mean
Qwen1.5-MoE A2.7B	Dense	-	78.61	38.80	4.57	32.93	60.96	43.17
	Wanda-sp	20	57.46	0.00	5.87	0.61	2.12	13.21
	FLAP	20	75.76	5.20	5.04	5.49	9.10	20.12
	Týr	20	73.77	14.00	3.24	7.32	39.96	27.66
	POP (Ours)	20	79.49	32.60	5.26	32.93	60.20	42.1
	Wanda-sp	40	12.53	0.00	0.03	0.00	0.99	2.71
	FLAP	40	67.51	1.40	3.66	0.61	2.58	15.15
	Týr	40	33.56	0.00	3.57	0.00	1.90	7.81
	POP (Ours)	40	76.99	21.20	2.24	12.20	42.91	31.11
Qwen2 57B-A14B	Dense	-	82.13	60.00	0.64	51.83	79.99	54.92
	Wanda-sp	20	9.87	0.00	0.30	0.00	1.59	2.35
	FLAP	20	81.76	22.60	1.25	11.59	70.43	37.53
	POP (Ours)	20	81.81	59.60	0.72	48.17	79.45	53.95
	Wanda-sp	40	0.18	0.00	0.03	0.00	1.74	0.39
	FLAP	40	66.15	1.00	1.77	0.61	16.76	17.26
	POP (Ours)	40	81.77	56.80	1.61	47.56	81.58	53.86
Qwen3 30B-A3B	Dense	-	81.70	73.00	12.08	32.93	89.16	57.77
	Wanda-sp	20	53.71	0.40	1.14	3.66	19.64	15.71
	FLAP	20	0.00	0.00	0.00	0.00	0.00	0
	Týr	20	79.75	45.60	4.96	20.73	64.29	43.07
	POP (Ours)	20	80.84	66.40	8.37	45.73	88.48	57.96
	Wanda-sp	40	6.82	0.00	0.06	0.61	0.23	1.54
	FLAP	40	0.00	0.00	0.00	0.00	0.00	0
	Týr	40	58.65	7.00	2.16	6.10	5.46	15.87
	POP (Ours)	40	79.85	28.60	1.77	15.24	67.78	38.65

Table 21. Detailed Accuracies (%) of Qwen2-VL (Wang et al., 2024) and Qwen2.5-VL (Bai et al., 2025) for 5 Visual Question Answering (VQA) tasks with different levels of structured sparsity. We used macro average as a mean value.

Model	Method	PR(%)	POPE	OK-VQA	GQA	ScienceQA	MME	Mean
Qwen2-VL	Dense	-	88.38	52.21	62.43	85.48	621.79	62.14
	Wanda-sp	20	7.54	1.22	1.89	28.46	5.71	7.86
	FLAP	20	86.79	32.37	51.71	50.53	343.93	46.74
	POP (Ours)	20	88.67	45.68	60.73	82.76	611.79	59.94
	Wanda-sp	40	0.00	0.01	0.04	0.00	0.71	0.02
	FLAP	40	0.00	0.00	0.01	0.05	0.00	0.01
	POP (Ours)	40	87.99	32.06	58.13	73.14	569.64	54.33
Qwen2.5-VL	Dense	-	87.59	43.88	60.86	88.75	625.36	60.68
	Wanda-sp	20	1.93	5.75	6.80	3.51	15.71	3.71
	FLAP	20	68.42	37.27	37.16	59.63	285.00	42.53
	POP (Ours)	20	87.22	42.65	60.21	85.15	617.50	59.46
	Wanda-sp	40	0.00	0.00	0.00	0.00	0.00	0.00
	FLAP	40	0.00	0.00	0.00	0.00	0.00	0.00
	POP (Ours)	40	86.73	34.86	57.47	74.89	537.86	54.63

Table 22. Accuracies (%) of Llama-2 (Touvron et al., 2023) and Llama-3 (Dubey et al., 2024) for 5 Generative tasks with different pruning strategies.

Params	Method	PR	coqa	mbpp	nq_open	humaneval	gsm8k	Mean
Llama3.1-8B	Variant (1)	20	78.06	32.4	3.60	21.95	37.45	34.69
	POP (Ours)	20	79.70	39.20	3.82	23.78	40.33	37.37
	Variant (2)	20	78.10	43.2	5.60	24.39	43.44	38.95
Llama2-7B	Variant (1)	20	75.83	15.20	7.87	6.71	11.37	23.4
	POP (Ours)	20	76.46	16.20	9.78	7.93	10.24	24.12
	Variant (2)	20	76.99	19.80	14.57	9.76	11.68	26.56

Table 23. Ablation study on the effect of partition fraction in POP on QA tasks. Accuracies (%) are reported under a fixed pruning ratio.

Params	PF	BoolQ	RTE	HS	WG	ARC-e	ARC-c	OBQA	Mean
Llama2-7B	0.05	71.84	63.18	52.17	66.46	70.03	38.14	28.60	55.77
	0.10	72.63	63.54	53.42	67.72	71.13	39.59	29.40	56.78
	0.20	72.29	64.26	55.06	67.80	72.31	40.02	28.40	57.16
Llama3.1-8B	0.05	76.42	66.79	53.14	70.09	75.13	43.09	29.00	59.09
	0.10	77.28	63.90	54.68	70.88	76.22	44.20	30.20	59.62
	0.20	79.14	67.15	57.05	71.43	78.87	49.23	33.20	62.3
Qwen3-8B	0.05	84.34	74.01	50.13	64.33	76.31	47.10	30.20	60.92
	0.10	84.77	74.37	51.76	64.80	77.78	48.21	28.80	61.5
	0.20	85.41	74.37	51.76	64.80	78.83	52.05	30.60	63.05

Table 24. Ablation study on the effect of partition fraction in POP on generative tasks. Accuracies (%) are reported under a fixed pruning ratio.

Params	PF	CoQA	MBPP	NQ-open	HumanEval	GSM8K	Mean
Llama2-7B	0.05	77.14	15.00	9.00	8.54	11.22	24.18
	0.10	76.46	16.20	9.78	7.93	10.24	24.12
	0.20	76.65	18.20	12.44	9.15	10.77	25.44
Llama3.1-8B	0.05	78.47	29.00	35.40	3.42	25.00	34.26
	0.10	79.70	39.20	3.82	23.78	40.33	37.37
	0.20	78.63	43.40	6.59	28.05	42.46	39.83
Qwen3-8B	0.05	80.73	52.20	1.19	53.66	85.29	54.61
	0.10	81.05	56.00	2.35	56.10	85.14	56.13
	0.20	80.01	61.80	4.32	57.32	84.91	57.67